Updated July 31st, 2005

Chapter III Printed Slot Antenna

Contents

3.1. On the microstrip feed model

Despite the significant amount of work on the modeling of the coaxial probe feed with the voltage gap sources, there is not much available from the literature with regard to exciting the microstrip line with a possible analog of the voltage gap. Putting the voltage gap directly on the microstrip line is mentioned in [1] and [2]. In [2], the gap is placed somewhere in the middle of the microstrip. In the Ansoft HFSS note [3], the microstrip feed is modeled by a finite perfect *H*-boundary that has a predefined voltage and the related *E*-field along the impedance line - the lumped port from the ground plane to the microstrip. This is one of two available methods (together with the wave port) in Ansoft HFSS to feed the microstrip. We note that the microstrip length should approximate half wavelength for a lumped load in order to avoid impedance transformation [4]. For distributed loads, this value may vary.

In the code example of Section 3.2, a long narrow microstrip (somewhat shorter than the half wavelength [5]) will be connected to the ground at the end of the substrate by a metal via strip. The feeding edge is chosen as the bottom edge of this via strip.

A simple test with the present code shows that the exact position of the feeding edge on an unloaded thin microstrip does not really matter: the results for the one-port network's input impedance indicate differences of about 1% when the feed is placed either on the via, on various edges of the microstrip, or elsewhere.

One must emphasize that the direct-connection model becomes inaccurate for wide microstrips and shall not be used in these cases. A more accurate microstrip port model is currently programmed. The microstrip mesh is also important for accurate results close to the microstrip edges. This in contrast to the approaches based on the Green's function for an infinite dielectric substrate, where no special meshing for the microstrip is necessary.

3.2. Microstrip-fed printed slot antenna (21 % bandwidth, $\varepsilon_r = 4.4$)

a. Geometry

This example describes a linearly-polarized microstrip-fed wide-slot broadband antenna at 1.67 GHz on a FR4 substrate with $\varepsilon_r = 4.4$ and the thickness of 0.8 mm [5]. The antenna geometry is shown in Fig. 3.1.

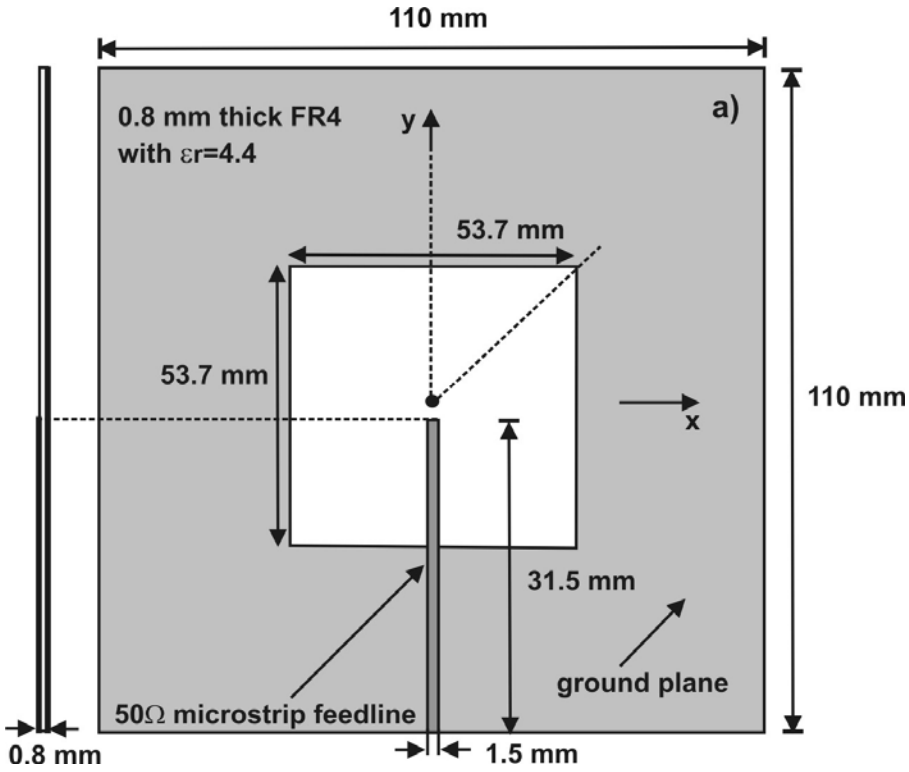

Fig. 3.1. Microstrip-fed rectangular-slot antenna at 1.67 GHz on a thin FR4 substrate [5].

The antenna has the following features:

1. The wide slot is feed by a 50 Ω microstrip line of the width 1.5 mm (see [4] for the characteristic impedance of the microstrip line), which is printed on the opposite side of the microwave substrate and placed symmetrically with respect to the centerline of the slot.
2. The printed slot antenna without a reflecting plane is a bi-directional radiator (the maximum gain occurs in the vertical direction). Current methods for reducing the back radiation of slot antennas use a metallic reflector or an enclosed cavity behind the slot [6, 7].

The microstrip end is offset from the slot center as shown in Fig. 3.1 in order to provide the impedance matching [5]. The microstrip feed is a voltage gap connector between the ground plane and the microstrip discussed above.

b. Code

For the corresponding MATLAB code please refer to http://ece.wpi.edu/mom/ and download `example31.zip`. The code should replicate Figs. 1-7 of this Chapter. In order to check the code functionality one may follow operations listed in Table 1 either in full or partially.

Table 1. Summary of operations to create and model a patch antenna with the probe feed.

Operation	Commands
Mesh generation **`1_mesh`**	1. Run `struct2d.m` and press the `Accept mesh` button to erase the existing antenna mesh 2. Run `struct3d.m` and - Press `OK` on the first (layer) GUI - Keep all tetrahedra in the mesh (Press `DONE`) - Select only the microstrip while selecting **metal faces of the ground plane** (bottom metal faces). Press `DONE` - When selecting **via metal patches** select only one edge – the bottom edge of the microstrip. Use the `Zoom In` option first. Then, draw a rectangle around this edge and `Close` it. The selected edge becomes blue. Press `DONE.` - Repeat the same operation for the **feed edge**. - When selecting **top metal faces** draw a multi-line polygon (or a number of polygons) that include all metal patches except the slot. `Close` every polygon. The selected metal patches become white. Use individual selection if for some reason the results are incorrect. Press `DONE`, then `OK` on the `Remove` screen. - Inspect the mesh visually.
BF generation **`2_basis`**	Run `wrapper.m` and inspect the resulting number of unknowns.
MoM solution **`3_mom`**	1. Open `impedance.m`. The frequency range and the number of discrete points are given in this file. Run `impedance.m`. 2. Run `comp_s.m` to inspect the antenna return loss. 3. Run `radpattern.m` to obtain the patterns (RHCP/LHCP) in the *H*-plane. 4. Run `nearfield.m` to inspect the field/charge/current distribution in the slot antenna.

c. Mesh

Fig. 3.2 shows the slot antenna mesh obtained after the mesh generation operation with `struct3d.m`. The final surface/volume mesh is also inspected with the script `struct3d.m`. Special attention should be paid to the feed assembly. The microstrip-line feed is modeled by connecting the ground plane and the 50 Ω microstrip line at the end of the substrate by a vertical metal strip of the same thickness with a voltage gap. This model is only applicable to the long narrow strips.

d. Input impedance

The antenna input impedance $Z_A = R_{in} + jX_{in}$ is calculated in the script `impedance.m` at the discrete frequency steps; it is a lengthy process. The present antenna mesh has 2836 unknowns, and the running time per frequency step is about 10 seconds. The antenna resonance occurs when the reactance X_{in} becomes zero at a certain frequency. The resonant frequency is close to 1.67 GHz.

The return loss (magnitude of the antenna reflection coefficient vs. 50 Ω) is calculated in the script `comp_s.m`. Note that the MATLAB figure shows the negative values for the return loss. The impedance bandwidth (for a narrowband antenna, e.g. for this antenna) is estimated as the length of the frequency domain where the return loss falls below 10 dB vs. the antenna center frequency. The estimation for the present antenna gives a value of 21%, which is large compared to the patch antenna. Fig. 3.3 shows the output of the script `comp_s.m`, which calculates the antenna return loss (dotted curve) compared to the return loss measured in Ref. [5] – shown by a solid curve. The dashed curve is the return loss when the number of MoM unknowns increases to 3782. One can see a reasonably good agreement.

The antenna center frequency is the frequency at which the return loss attains its maximum value. This value is also close to 1.67 GHz.

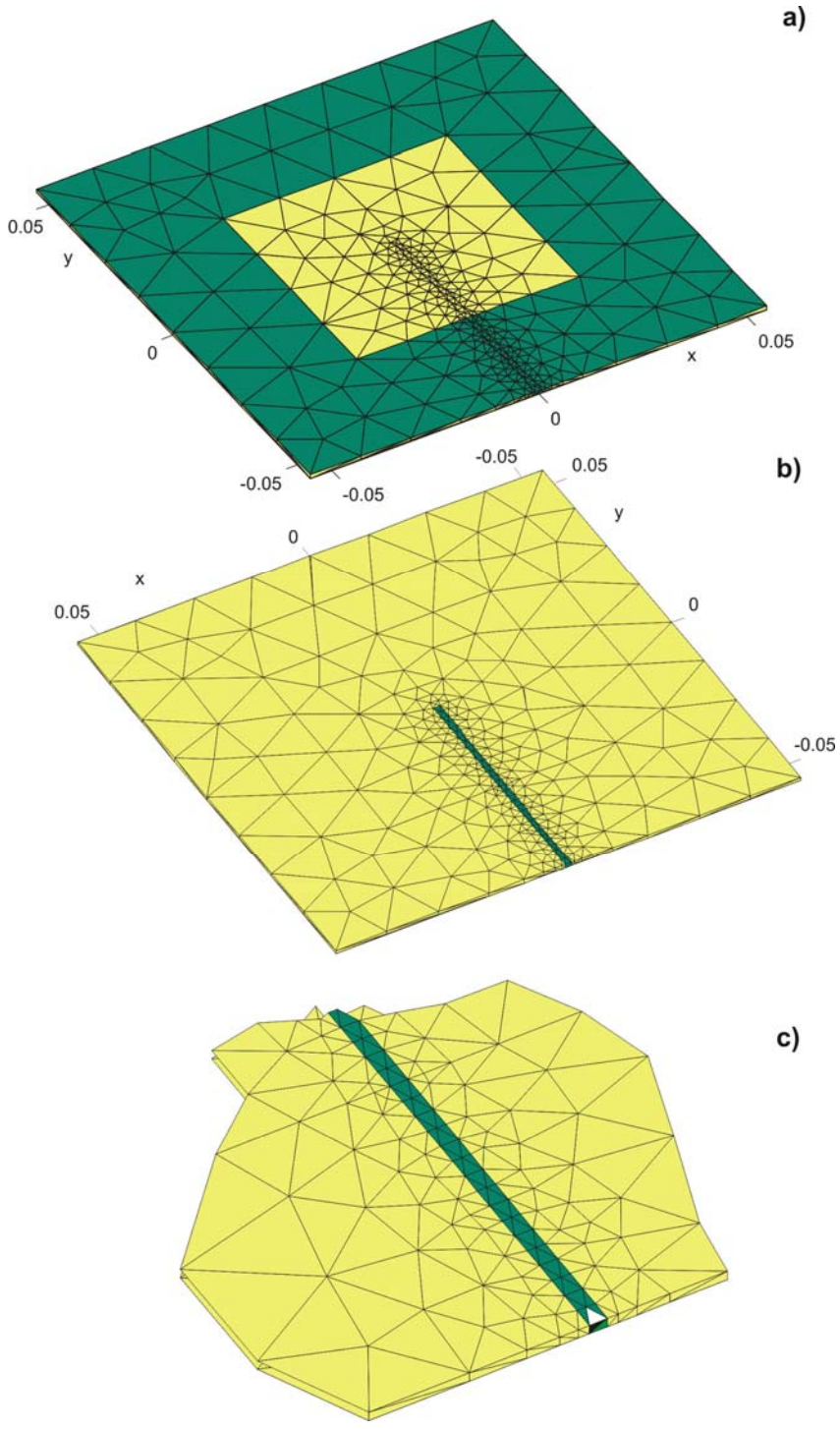

Fig. 3.2. a) – Slot antenna – top view. The dielectric faces are shown by a light color; b) – bottom view of the slot antenna; c) – enlarged feed domain. The feed basis function is marked by white and black triangles.

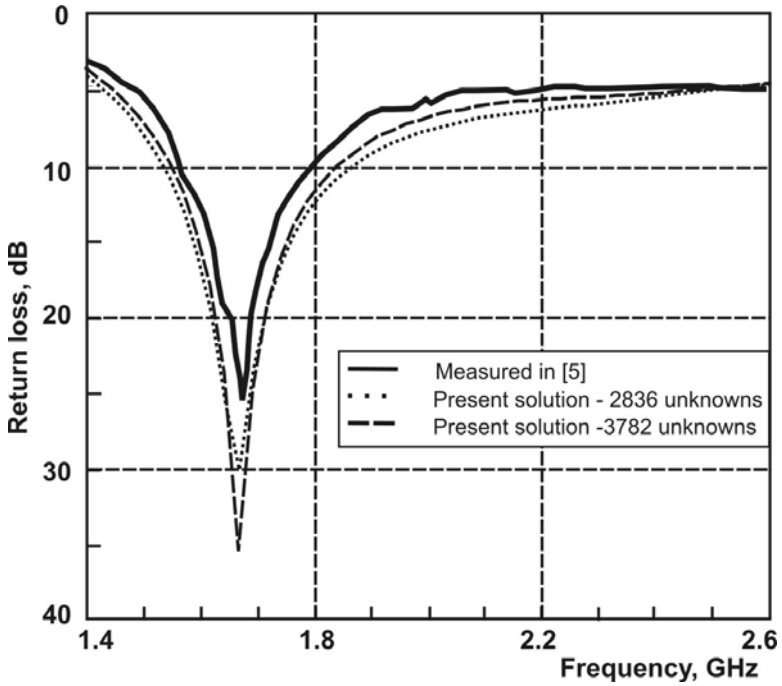

Fig. 3.3. Return loss of the slot antenna as a function of frequency. Solid curve – measurements [5]; dotted curve – present solution with 2836 unknowns; dashed curve – present solution with 3782 unknowns.

e. Radiation pattern – total directivity/gain

The radiation characteristics are calculated in the script `radpattern.m` – see Section 2.1 of Chapter II for a description of that script. The script accepts a frequency value, searches for the closest MoM solution saved in the file `out.mat` (output of `impedance.m`) and then calculates the electric and magnetic fields based on this solution – see Section 7.3 of Chapter VII. The directivity plot over the sphere surface (script `radpattern.m`) for the present antenna is shown at the resonance (1.67 GHz) in Fig. 3.4.

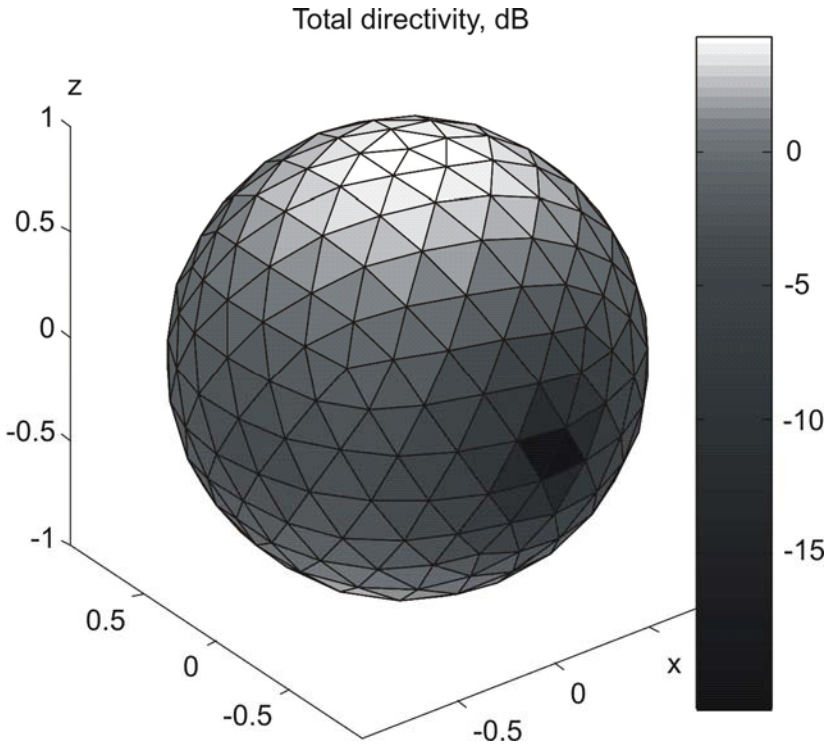

Fig. 3.4. Total directivity for the patch antenna shown in Fig. 3.1 at the resonance. The maximum directivity (maximum gain in this lossless case) is approximately 4.5 dB at zenith.

The script `radpattern.m` gives a relative difference of 0.74% between the radiated and the feed power in the present case.

f. Radiation pattern – co-polar and cross-polar components

The co-polar and cross-polar directivity components are found similar to the approach described in Section 2.1. Here, we are interested in the *H*-plane radiation patterns (the *xz*-plane) for the present configuration.

The script `radpattern.m` outputs two radiation patterns for the present antenna, in the *H*-plane (the *xz*-plane in our case). In this plane, the cross-polarization directivity dominates. The offset for the MATLAB polar plot is given as 35 dB. Fig. 3.5a compares the radiation patterns in the *H*-plane with the measurement [5]. One can see a reasonably good agreement. The corresponding comparison for the *E*-plane is given in Fig. 3.5b.

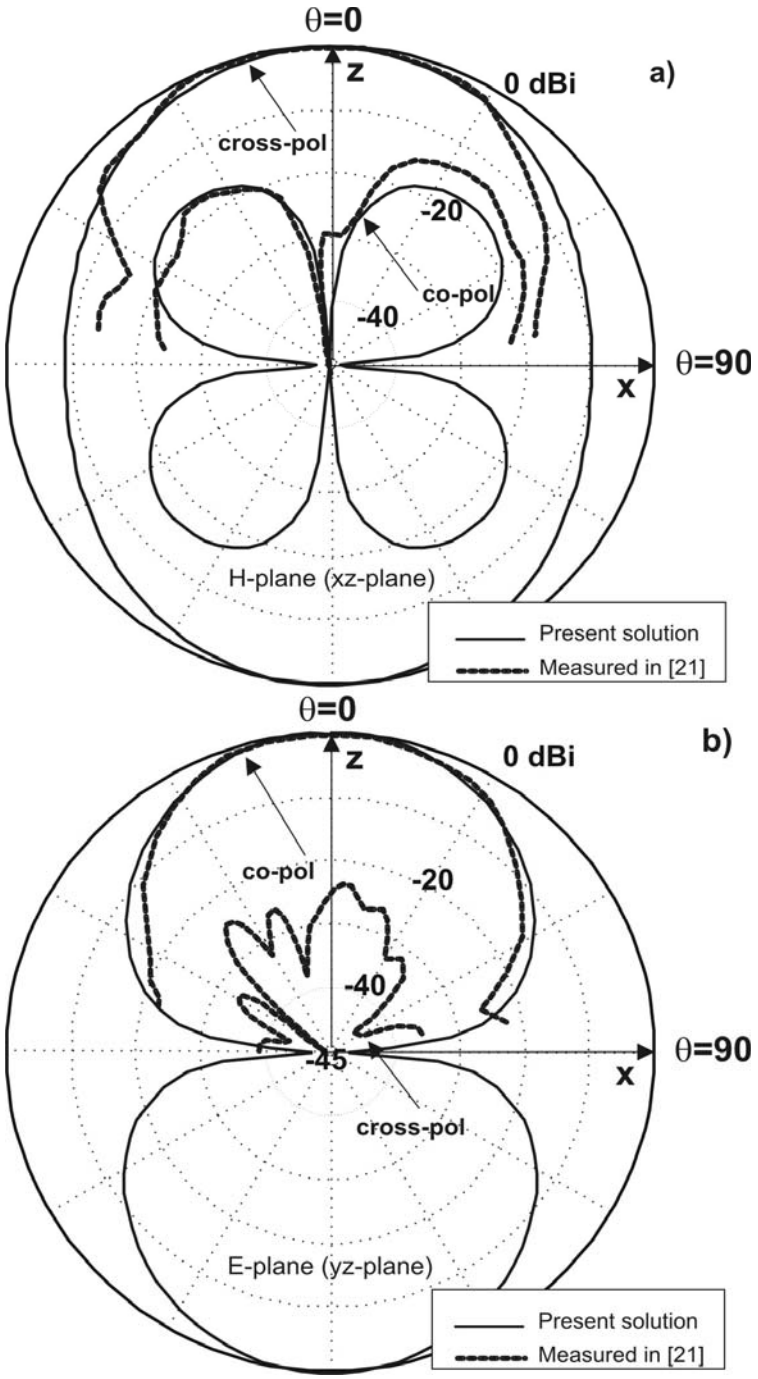

Fig. 3.5. Normalized directivity of the co-polar and cross-polar fields vs. elevation angle for the slot antenna [5], at the resonant frequency, in the *H*- and *E*-planes, respectively. The coarsest MoM mesh with 2836 unknowns is used. The MoM solution is shown by a solid curve; the experimental data [5] is given by dashed curves. The MoM cross-polarization is below 45 dBi in the *E*-plane and is therefore not seen in Fig. 3.5.

g. Near fields

It is desired to inspect the near field distributions in the antenna volume or on the antenna surface. The script `nearfield.m` finds and displays such distributions at a given frequency. The script accepts a frequency value, searches for the closest MoM solution saved in the file `out.mat` (output of `impedance.m`) and then calculates the electric and magnetic near fields based on this solution – see Section 7.3 of Chapter VII. The fields are calculated at the center of every tetrahedron in the dielectric mesh. The bound surface charge density on the dielectric surface is found using the MoM solution. Next, the electric current density on the metal surface and the associated free charge distribution are found using the MoM solution for the metal patches. Fig. 3.6 shows two such distributions for the present antenna; the Poynting vector density in the dielectric and the surface current density on the metal surface. It is seen in Fig. 3.6 how the energy is supplied to the cavity using the microstrip.

h. Other scripts

The script `eigenfreq.m` in the folder 3_mom is intended for the eigenfrequency search. It will not run for the present antenna configuration. To find the eigenfrequencies of the corresponding TM resonator one needs to go back to the folder `1_mesh` and create the same structure, but without the antenna feed (do not select the metal via patches for the feed, and do not select the feeding edges). Then, one creates the basis functions and runs `eigenfreq.m` in order to find the resonant frequency and the *Q*-factor of the corresponding resonator.

The output of the script `eigenfreq.m` is shown in Fig. 3.7. Note that the cavity resonance strongly depends on the presence of the microstrip and disappears if the microstrip is removed. The resonator frequency found in this way (about 1.57 GHz) is lower than the antenna center frequency. A finer mesh around the slot cavity may be necessary to reduce the difference. The *Q*-factor is about 5.6, which is a rather small value. Accordingly, the antenna impedance bandwidth is large – 21%. In the present case, the impedance bandwidth approximately agrees with the estimate $B \approx 1/Q$ discussed in Chapter II.

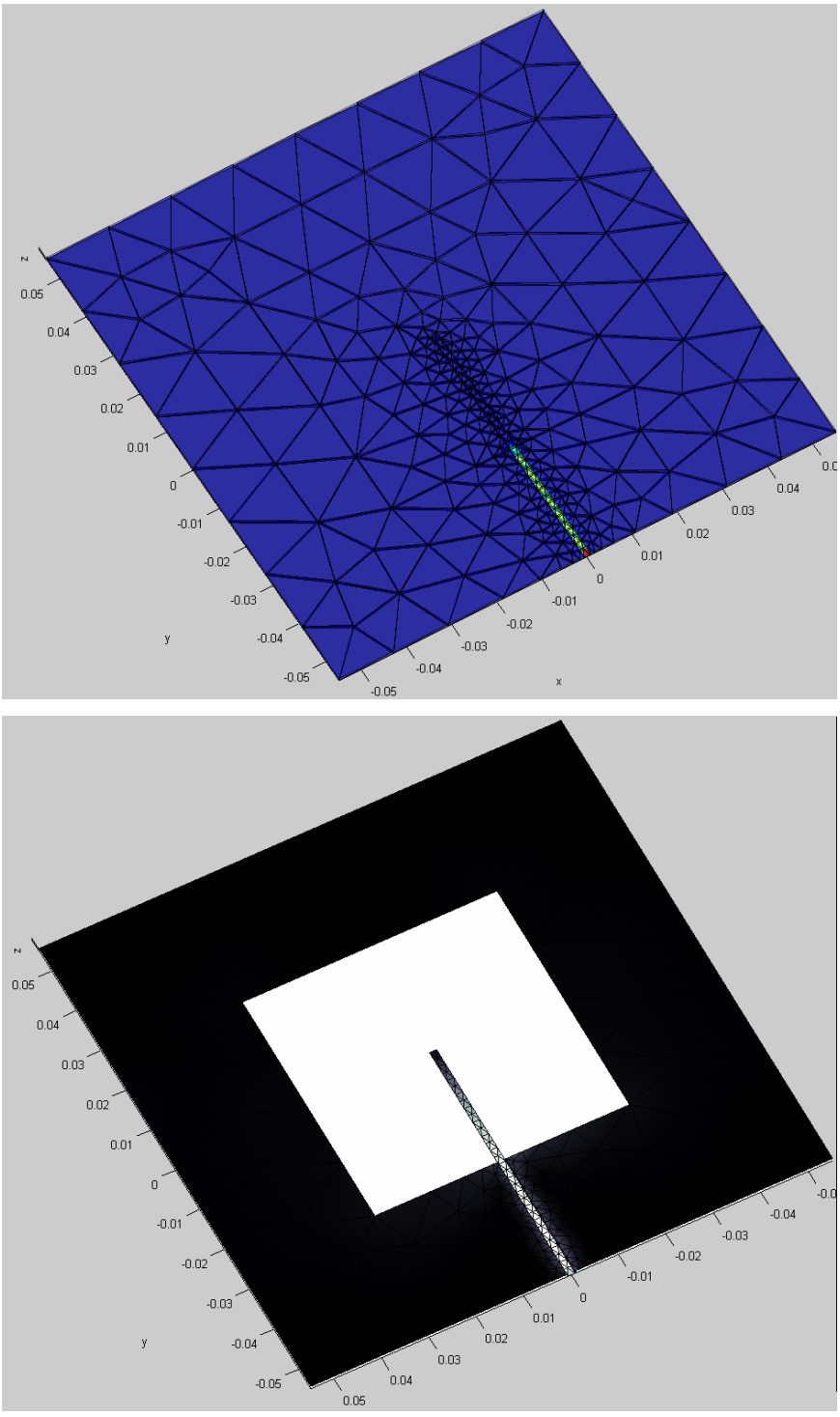

Fig. 3.6. Fields within the slot antenna at the resonant frequency. Top – Poynting vector (magnitude distribution) within the dielectric tetrahedra. Redder hues (which have lighter colors) correspond to the larger power density magnitudes. Bottom – electric current (magnitude) distribution on the metal surface (bottom view).

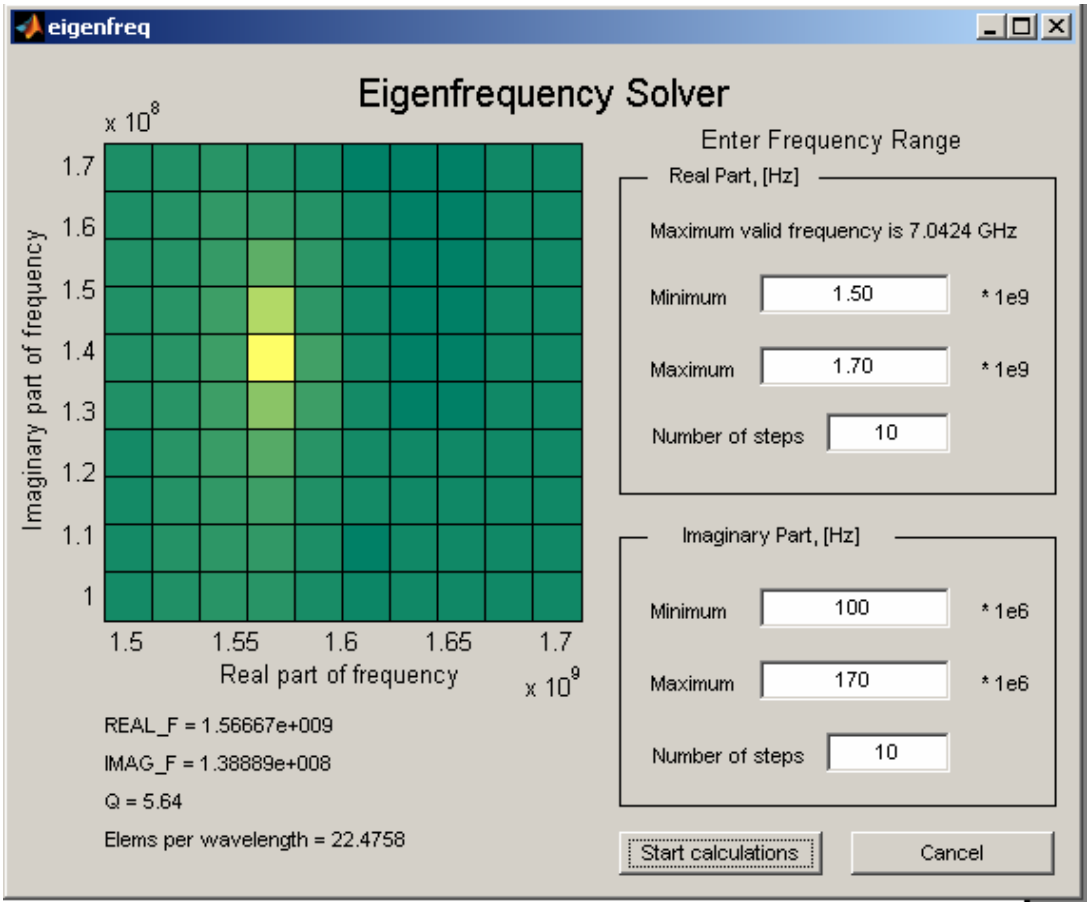

Fig. 3.7. Resonant frequency and the *Q*-factor of the slot antenna cavity. The feed strip is removed from the antenna mesh, which includes only the microstrip, the slotted top metal plane, and the dielectric.

3.3. Crossed-slot cavity-backed circularly polarized antenna (2.0% bandwidth)

a. Geometry

This example describes a circularly-polarized crossed-slot antenna at 2.34 GHz [7] on a high-frequency Rogers RT/duroid® 5880 laminate [8] with $\varepsilon_r = 2.20$ and a thickness of 3.0 mm. A crossed-slot multimode antenna at 2.34 GHz from Ref. [7] is intended for satellite digital audio radio service and needs to be circularly-polarized over most of the upper hemisphere, but vertically-polarized near the horizon. The antenna geometry with two crossed slots of a slightly different length is shown in Fig. 3.8. Since the probe feed thickness is not reported, a metal column of cross-section 0.5×0.5 mm was chosen here.

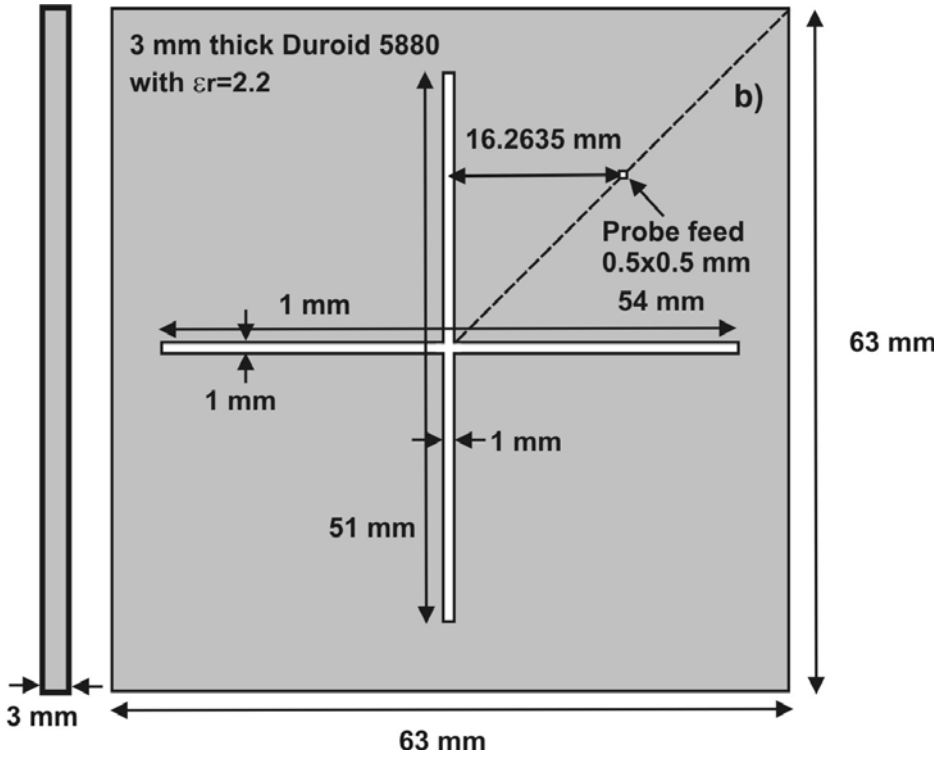

Fig. 3.8. Crossed-slot probe-feed CP antenna from Ref. [7].

The antenna has the following features:

1. The cavity provides the role of the reflector for the slot antenna. However, the front-to-back ratio still remains relatively poor (see below) unless a large metal ground plane is introduced [7].
2. The dielectric cavity filling is intended to reduce the cavity size.

3. A number of different cavity TEM modes may be excited in this configuration [7].

b. Code

For the corresponding MATLAB code please refer to http://ece.wpi.edu/mom/ and download `example25.zip`. The code should replicate Figs. 9-13 of this Chapter. In order to check the code functionality one may follow the steps listed in Table 1 at the beginning of Section 3.1 either in full or partially. The antenna structure is created similarly to the slot antenna structure in Section 3.1. To create the metal cavity, all border edges of the base planar mesh should be selected as via. The creation of the feed is similar to the patch antenna feed considered in Section 3.1. The dielectric tetrahedra must be removed from the feed. One significant difference is, however, in the feed location, which is altered in the script `feed.m`.

c. Mesh

Fig. 3.9 shows the slot antenna mesh obtained after the mesh generation operation. The final surface/volume mesh is inspected with the script `struct3d.m`. Special attention should be paid to feed assembly (selecting the via patches for the feed column, and identifying the feeding edges). The visual feed inspection is also done with `struct3d.m`.

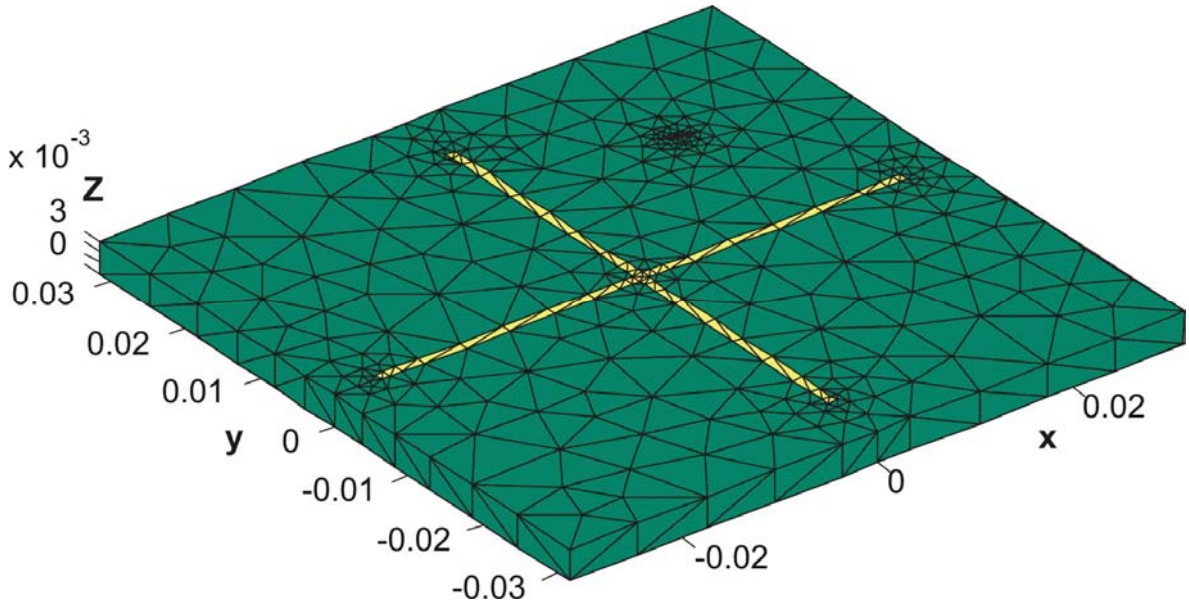

Fig. 3.9. Volume/surface mesh for the slot antenna created by `struct3d.m`. The dielectric (inside the metal cavity) is shown by lighter color. The feed column inside the cavity is not seen.

d. Input impedance

The antenna input impedance $Z_A = R_{in} + jX_{in}$ is calculated in the script `impedance.m` at the discrete frequency steps. The number of steps and the frequency range are specified in that script. The present antenna mesh has 4578 unknowns and needs about 37 seconds per frequency step on a PIV 3.6 GHz (double precision).

The return loss (magnitude of the antenna reflection coefficient vs. 50 Ω) is calculated in the script `comp_s.m`. Note that the MATLAB figure shows the negative values for the return loss. The impedance bandwidth (for a narrowband antenna, e.g. for the present antenna) is estimated as the length of the frequency domain where the return loss falls below 10 dB vs. the antenna center frequency. The estimation for the present antenna gives a value of about 4.3%. The antenna center frequency is the frequency at which the return loss attains its maximum value. This value is also close to 2.34 GHz. Fig. 3.10 shows the output of the script `comp_s.m`, which compared the MoM return loss data with the corresponding experimental data [7].

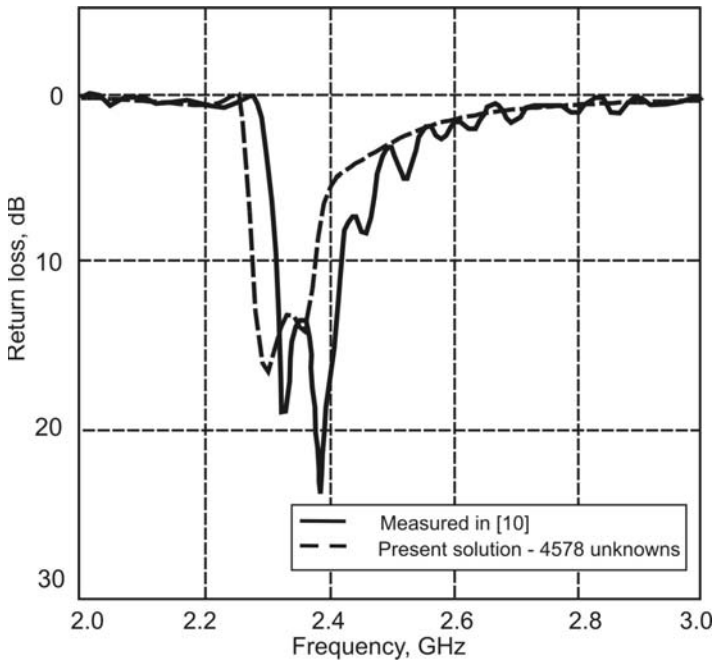

Fig. 3.10. Return loss as a function of frequency for the crossed-slot probe-fed CP antenna (from Ref. [7]). Solid curve – measurements [7]; dashed curve – present solution with 4578 unknowns.

In the MATLAB example code, a frequency range smaller than that in Fig. 3.10 has been chosen. This is done to avoid a more lengthy simulation that was required for Fig. 3.10.

e. Radiation pattern – total directivity/gain

The radiation characteristics are calculated in the script `radpattern.m` – see Section 2.1 for a description of that script. The script accepts a frequency value, searches for the closest MoM solution saved in the file `out.mat` (output of `impedance.m`) and then calculates the electric and magnetic fields based on this solution – see Section 7.3 of Chapter VII. The directivity plot over the sphere surface (script `radpattern.m`) for the present antenna is shown at the resonance in Fig. 3.11.

The script `radpattern.m` gives the relative difference of 0.81% between the radiated and the feed power in the present case.

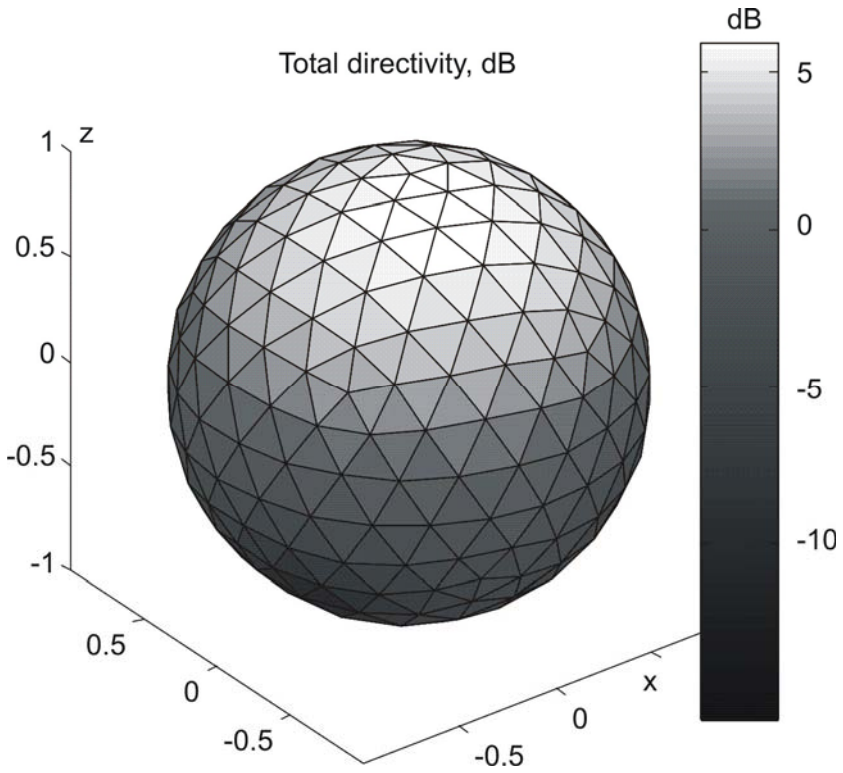

Fig. 3.11. Total directivity of the slot antenna at 2.34 GHz.

f. Radiation pattern – RHCP and LHCP components

The radiation patterns are measured in [7] by mounting the antenna on a metallic pedestal and then placing it in the center of a 1m×1m ground plane. The measured results

averaged over four elevation planes are shown in Fig. 3.12a, b, respectively. Since we are not able to reproduce these conditions exactly, only the free-space simulated radiation patterns are presented here (Fig. 3.12c, d).

Once the spherical components E_θ, E_ϕ of the electric field in the script `radpattern.m` are known (see Section 2.1) the right-handed circular polarization component (RHCP) and the left-handed circular polarization component (LHCP) of the electric field are given by

$$E_{\text{RHCP}} = \frac{1}{\sqrt{2}}\left(E_\theta + jE_\phi\right)$$
$$E_{\text{LHCP}} = \frac{1}{\sqrt{2}}\left(E_\theta - jE_\phi\right) \tag{3.1}$$

Then, the RHCP directivity yields

$$D_{\text{RHCP}}(\vec{r}) = 10\log_{10}\left(\frac{4\pi R^2 W}{P_{\text{rad}}}\right), \quad W = \frac{1}{2\eta}\left|E_{\text{RHCP}}\right|^2 \tag{3.2}$$

for any fixed large radius *R*. Similarly, the LHCP directivity gives

$$D_{\text{LHCP}}(\vec{r}) = 10\log_{10}\left(\frac{4\pi R^2 W}{P_{\text{rad}}}\right), \quad W = \frac{1}{2\eta}\left|E_{\text{LHCP}}\right|^2 \tag{3.3}$$

Both polarizations are found in the script `radpattern.m` and are plotted in Fig. 3.12c at 2.34 GHz. One can see that RHCP dominates by only 7 dB at zenith. However, the polarization isolation is not very significant and a considerable back lobe is observed. This means that noise from the backside of the antenna will be present in the spectrum of the received signal.

While the cross-polarization isolation of about 10 dB toward zenith reported in [7] is to a certain extent confirmed in Fig. 3.12c, the vertical polarization is essentially missing for the antenna without the ground plane as shown in Fig. 3.12d. It follows from

here that the present antenna setup may not be used without a sufficiently large ground plane.

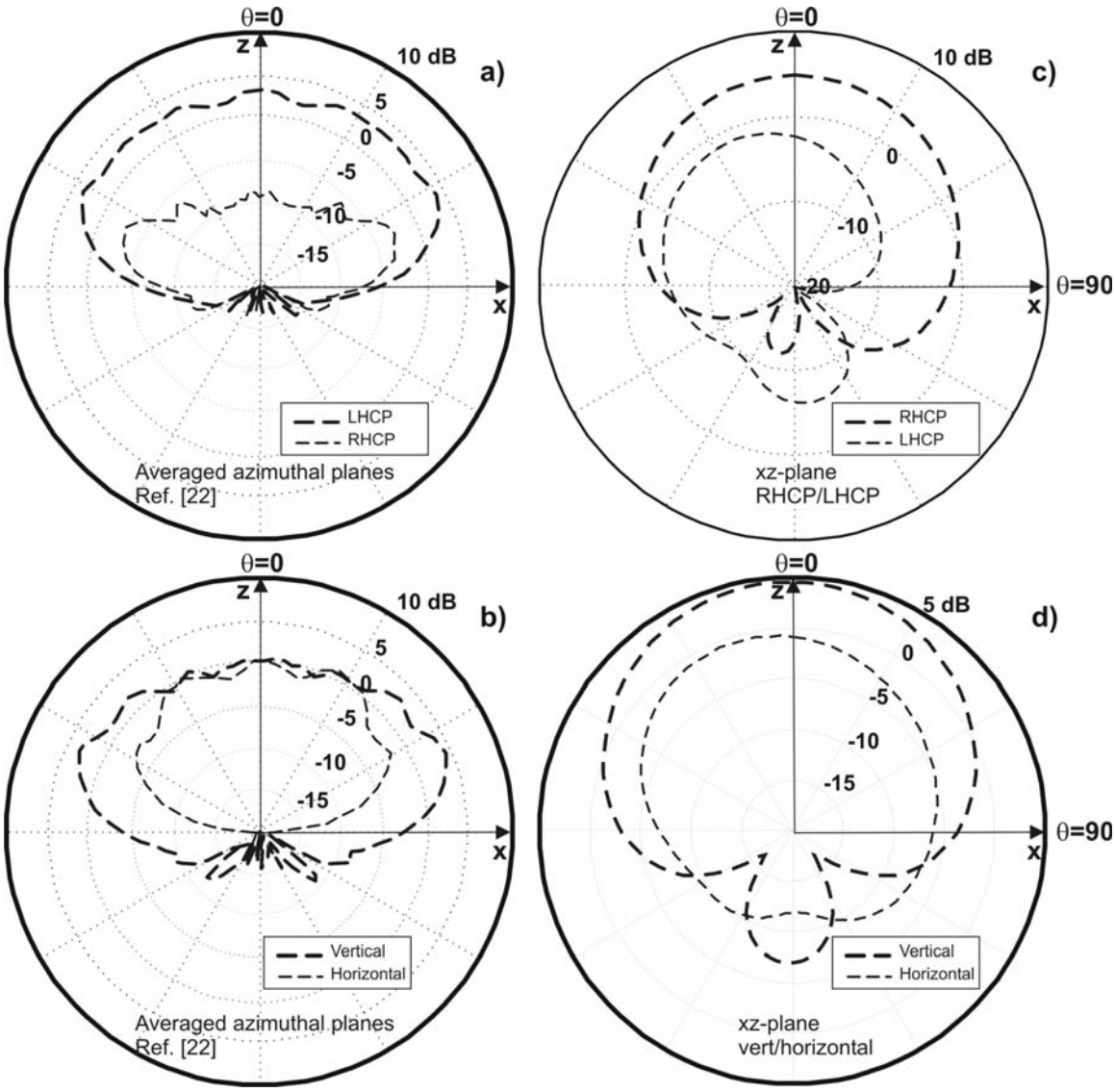

Fig. 3.12. Absolute directivity of the LHCP/RHCP and co-/cross-polar fields vs. elevation angle for the slot antenna [7], at the resonant frequency of 2.34 GHz, in the *xz*-plane. a), b) – averaged over azimuthal angle experimental results [7] with a pedestal and a large ground plane; c), d) present solution for a free-space radiation – for circular (c) and linear (d) polarization, respectively.

g. Near fields

It is desired to inspect the near field distributions in the antenna volume or on the antenna surface. The script `nearfield.m` finds and displays such distributions at a given frequency. The script accepts a frequency value, searches for the closest MoM solution saved in the file `out.mat` (output of `impedance.m`) and then calculates the electric and magnetic near fields based on this solution – see Section 7.3 of Chapter VII. The fields are calculated at the center of every tetrahedron in the dielectric mesh. The bound surface charge density on the dielectric surface is found using the MoM solution. Next, the electric current density on the metal surface and the associated free charge distribution are found using the MoM solution for the metal patches. Fig. 3.13 shows the bound surface charge density at two frequencies: 2.30 GHz (lower band frequency) and 2.39 GHz (upper band frequency). The field inspection within the antenna indicates the typical TM "dipole" mode at 2.30 GHz (lower frequency band) in the slotted cavity volume, but a less common quadrupole mode is excited at 2.39 GHz (upper frequency band). Both these modes were observed in Ref. [7] using Ansoft HFSS.

h. Other scripts

The script `eigenfreq.m` in the folder 3_mom is intended for the eigenfrequency search. It will not run for the present antenna configuration. To find the eigenfrequencies of the corresponding TM resonator one needs to go back to the folder `1_mesh` and create the same structure, but without the antenna feed (do not select the metal via patches for the feed, and do not select the feeding edges). Then, create the basis functions and run `eigenfreq.m` in order to find the resonant frequency and the *Q*-factor of the corresponding resonator. The eigenmode resonances for this example were not specifically calculated.

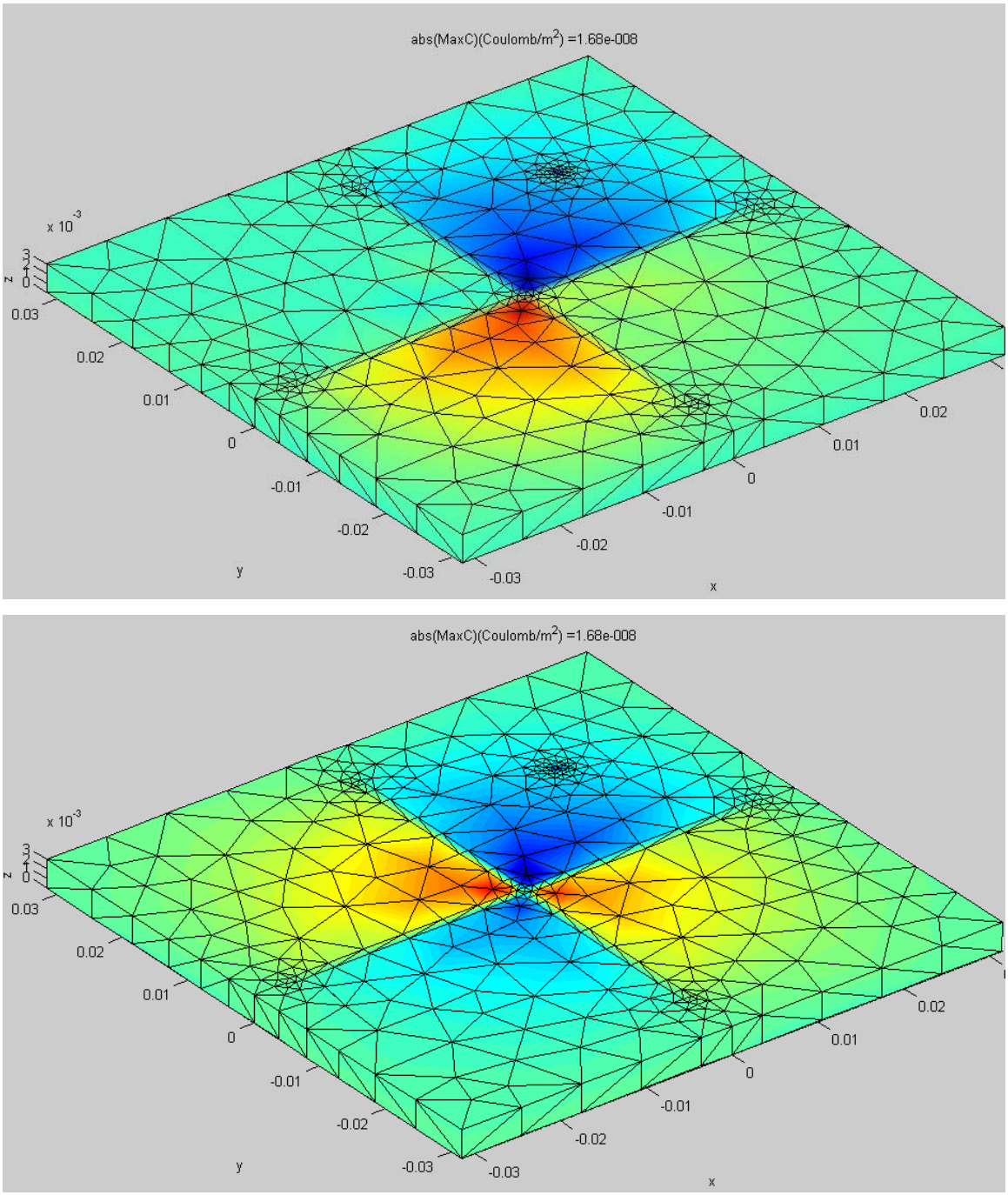

Fig. 3.13. Fields within the slot antenna. Top – surface bound charge distribution at 2.30 GHz; bottom – the same distribution at 2.39 GHz. Redder hues correspond to positive charge, bluer hues to negative charge.

References

1. L. Matekovits, G. Vecchi, P. Pirinoli, and M. Orefice, "Network parameters of printed antennas from the MoM solution," In: *International Sym. Antennas and Propagation*, 1998. IEEE, vol. 4, pp. 1838 – 1841, 21-26 June 1998.
2. B. G. Salman and A. McCowen, "The CFIE technique applied to finite-size planar and non-planar microstrip antenna," *Third International Conference on Computation in Electromagnetics*, 1996. Conf. Publ. No. 420, 10-12, pp. 338 - 341, April 1996.
3. Application note "*Gap Model*", Ansoft Corp. , 2001**.** Available online: ftp://ftp.ansoft.com/techsup/download/web/ftproot_inet/products/hfss/faqs/portmicrostrip.htm.
4. D. M. Pozar, *Microwave Engineering*, Wiley, New York, 2005, third edition.
5. J.-Y. Sze and K.-L. Wong, "Bandwidth enhancement of a microstrip-line-fed printed wide-slot antenna**,**" *IEEE Trans. Antennas and Propagation*, vol. AP-49, no. 7, pp. 1020-1024, July 2001.
6. R. Qinjiang and T. A. Denidn, "A single-substrate microstrip-fed slot antenna array with reduced back radiation," *Antennas and Wireless Propagation Letters*, vol. 3, no. 1, pp. 265-268, 2004.
7. D. Sievenpiper, H.-P. Hsu, and R. M. Riley, "Low-profile cavity backed crossed-slot antenna with a single probe feed designed for 2.34-GHz Satellite Radio applications," *IEEE Trans. Antennas and Propagation*, vol. AP-52, no. 3, pp. 873-879, March 2004.
8. A summary of Rogers laminates can be found at http://www.secomtel.com/UpFilesPDF/PDF/ROGERS/rt312.pdf